

Rising bosonic electroweak virtual effects at high energy e^+e^- colliders

M. Beccaria

*Dipartimento di Fisica, Università di Lecce and INFN, Sezione di Lecce
Via Arnesano, 73100 Lecce, Italy*

G. Montagna and F. Piccinini

*Dipartimento di Fisica Nucleare e Teorica, Università di Pavia and INFN, Sezione di Pavia
Via A. Bassi 6, 27100 Pavia, Italy*

F.M. Renard

*Physique Mathématique et Théorique, UMR 5825
Université Montpellier II, F-34095 Montpellier Cedex 5.*

C. Verzegnassi

*Dipartimento di Fisica, Università di Lecce and INFN, Sezione di Lecce
Via Arnesano, 73100 Lecce, Italy
(August 8, 2018)*

The virtual massive gauge boson effects on several observables in the process of charged fermion pairs production at e^+e^- colliders are computed up to the TeV energy range in the Standard Model, working in the “Z-peak subtracted” representation. It is shown that these effects increase regularly with energy, approaching the typical ten percent relative size. A careful numerical evaluation is proposed, where the conditions dictated by gauge invariance are consistently implemented.

12.15.Lk,13.10.+q,13.40.K,13.60.Hb

I. INTRODUCTION

The accurate computation of virtual electroweak effects has appeared to be a fundamental theoretical contribution for a correct interpretation of the experimental results obtained in several years of running at the Z resonance at LEP1 and SLC [1]. Leaving aside the remarkable degree of accuracy to which the Standard Model (SM) has been tested at the one loop level, the prediction for the value of the top mass (spectacularly confirmed by its experimental discovery) and the subsequent limits on the “low” value of the Higgs mass undoubtedly represent an illustration of how relevant a rigorous calculation of virtual effects may be.

From a purely technical point of view, a calculation of electroweak (i.e. of not conventional QED type) virtual effects appears to be somehow simplified on top of the Z resonance, since for trivial reasons the non resonant terms can be evidently neglected. This eliminates the full set of “box” diagrams, thus reducing the theoretical task to that of computing self-energies and vertices. In the self-energies, the dominant effect is provided by light fermion pairs that determine the running of $\alpha^{(QED)}$ up to the Z mass [2], and by the heavy top that shifts from 1 the value of the ρ parameter [3].

A welcome feature of these fermionic contributions is that they are separately gauge independent. This is also true for what concerns the remaining “large” $\simeq m_t^2$ virtual effect provided by the $Zb\bar{b}$ vertex [4]. Therefore, the full set of “relevant” virtual electroweak contributions at the Z peak appears to be relatively “simple”, the main role being played by either the fermionic content of self-energies or by a gauge independent subset of the bosonic effects.

As soon as one moves away from the special LEP1/SLC configuration, the expectation is that the previous simple features might disappear. In particular, the role of boxes (where s -channel W exchange is intrinsically not gauge independent), could become much more relevant. Should this be the case, one extra immediate complication would arise since the gauge dependence e.g. of W bosons must be cancelled, in the contributions to physical observables, by that of suitable combinations of corresponding self-energies and vertices where virtual W s are exchanged. Clearly, only the sum of such special box, self-energies and vertices combinations can acquire a physical meaning, and must be computed as carefully as possible.

To make the previous discussion more quantitative, we can now provide one numerical example, i.e. the calculation of the box contribution to cross sections and asymmetries in the LEP2 energy range. Working in the t’Hooft $\xi = 1$ gauge, one sees [5] that, at the largest considered energy $\sqrt{s} \simeq 200$ GeV, the related effect can become quite respectable

(a relative one percent in the muon cross section and a two-three percent in the hadronic cross section). Since this effect is apparently increasing with energy, a question that naturally arises at this stage is that of whether this feature will remain valid, or stronger, at the future linear e^+e^- colliders, whose energies are expected to lie in the 500 GeV range (or more [6]). In particular, the problem that one should face is that of computing correctly the relevant gauge-invariant combinations of self-energies, vertices and boxes. In fact, if their size became “quite” respectable, the extra problem of the calculation of the initial-state QED radiation corrections should also be considered in a self-consistent way i.e. including all the various terms in the convolution process that is usually involved [7].

The aim of this paper is precisely that of computing, in a fully gauge invariant way, the contribution of bosonic effects to physical observables of e^+e^- annihilation into charged fermion pairs. This will be done in an energy range from 200 GeV to 1 TeV (although we could increase the upper limit if requested), working systematically in our chosen subtracted theoretical framework. As we shall see, the numerical effect generally increases with energy, approaching a typical ten percent size at the TeV scale. This will be fully discussed in the following Sec. II and Sec. III, where the numerical calculation of a few relevant observables will be performed without taking photon emission into account. The large size of the effect will then motivate a rigorous calculation of the initial-state QED radiation corrections; this will be treated in Sec. IV. A final brief discussion will then be given in the concluding Sec. V. An appendix contains explicit formulae that are involved in the procedure but not essential for a qualitative understanding of the main results.

II. BOSONIC VIRTUAL EFFECTS IN THE “Z-PEAK SUBTRACTED” REPRESENTATION

It has been recently shown [8,9] that the process of e^+e^- annihilation into fermion pairs, at squared center of mass (c.m.) energy q^2 larger than M_Z^2 , can be conveniently described using an effective parameterization, strictly valid at the one loop level, where only subtracted quantities appear as “electroweak corrections”. In particular, the contributions to all observables generated by the Z boson exchange are systematically subtracted on top of the Z peak, at $q^2 = M_Z^2$, in full analogy with the photon contributions that are subtracted “on top” of the photon peak at $q^2 = 0$. As a consequence of this procedure, the theoretical input in the various Z contributions will contain quantities (partial Z widths and asymmetries) measured at the Z resonance. These input parameters will replace the commonly used Fermi coupling G_μ , and we devote the interested reader to Refs. [8,9] for an exhaustive discussion of the details of the approach. The final result is that, in the complete expression of a general observable of the process $e^+e^- \rightarrow f\bar{f}$, there will be some “leading” terms containing α_{QED} , M_Z and Z peak observables and four independent one loop subtracted corrections that contain all the residual physical information and are defined as:

$$\tilde{\Delta}_{\alpha,ef}(q^2, \theta) = \tilde{F}_{\gamma\gamma,ef}(0, \theta) - \tilde{F}_{\gamma\gamma,ef}(q^2, \theta) \quad (2.1)$$

$$R_{ef}(q^2, \theta) = I_{Z,ef}(q^2, \theta) - I_{Z,ef}(M_Z^2, \theta) \quad (2.2)$$

$$V_{ef}^{\gamma Z}(q^2, \theta) = \frac{\tilde{A}_{\gamma Z,ef}(q^2, \theta)}{q^2} - \frac{\tilde{A}_{\gamma Z,ef}(M_Z^2, \theta)}{M_Z^2} \quad (2.3)$$

$$V_{ef}^{Z\gamma}(q^2, \theta) = \frac{\tilde{A}_{Z\gamma,ef}(q^2, \theta)}{q^2} - \frac{\tilde{A}_{Z\gamma,ef}(M_Z^2, \theta)}{M_Z^2} \quad (2.4)$$

In the previous expressions, we have used the following definitions:

$$I_{Z,ef}(q^2, \theta) = \frac{q^2}{q^2 - M_Z^2} [\tilde{F}_{ZZ,ef}(q^2, \theta) - \tilde{F}_{ZZ,ef}(M_Z^2, \theta)] \quad (2.5)$$

$$\tilde{A}_{ZZ,ef}(q^2, \theta) = \tilde{A}_{ZZ,ef}(0, \theta) + q^2 \tilde{F}_{ZZ,ef}(q^2, \theta) \quad (2.6)$$

$$\tilde{A}_{ZZ,ef}(q^2, \theta) = A_{ZZ}(q^2) - (q^2 - M_Z^2) [(\Gamma_{\mu,e}^{(Z)}, v_{\mu,e}^{(Z)}) + (\Gamma_{\mu,f}^{(Z)}, v_{\mu,f}^{(Z)}) + (q^2 - M_Z^2) A_{ZZ,ef}^{(Box)}(q^2, \theta)] \quad (2.7)$$

$$\tilde{F}_{\gamma\gamma,ef}(q^2, \theta) = F_{\gamma\gamma,ef}(q^2) - (\Gamma_{\mu,e}^{(\gamma)}, v_{\mu,e}^{(\gamma)}) - (\Gamma_{\mu,f}^{(\gamma)}, v_{\mu,f}^{(\gamma)}) - q^2 A_{\gamma\gamma,ef}^{(Box)}(q^2, \theta) \quad (2.8)$$

$$\begin{aligned} \frac{\tilde{A}_{\gamma Z,ef}(q^2, \theta)}{q^2} &= \frac{A_{\gamma Z}(q^2)}{q^2} - \left(\frac{q^2 - M_Z^2}{q^2}\right) (\Gamma_{\mu,f}^{(\gamma)}, v_{\mu,f}^{(Z)}) \\ &\quad - (\Gamma_{\mu,e}^{(Z)}, v_{\mu,e}^{(\gamma)}) - (q^2 - M_Z^2) A_{\gamma Z,ef}^{(Box)}(q^2, \theta) \end{aligned} \quad (2.9)$$

$$\begin{aligned} \frac{\tilde{A}_{Z\gamma,ef}(q^2, \theta)}{q^2} &= \frac{A_{\gamma Z}(q^2)}{q^2} - \frac{q^2 - M_Z^2}{q^2} (\Gamma_{\mu,e}^{(\gamma)}, v_{\mu,e}^{(Z)}) \\ &\quad - (\Gamma_{\mu,f}^{(Z)}, v_{\mu,f}^{(\gamma)}) - (q^2 - M_Z^2) A_{Z\gamma,ef}^{(Box)}(q^2, \theta) \end{aligned} \quad (2.10)$$

The quantities $A_{ij}(q^2) = A_{ij}(0) + q^2 F_{ij}(q^2)$ ($i, j = \gamma, Z$) are the conventional transverse γ, Z self-energies. $A_{\gamma\gamma, \gamma Z, Z\gamma, ZZ, ef}^{(Box)}(q^2, \theta)$ are the projections on the photon and Z Lorentz structures of the box contributions to the scattering amplitude \mathcal{A}_{ef} and the various brackets (Γ_{μ}, v_{μ}) are the projections of the vertices on the different Lorentz structures to which $\tilde{A}_{\gamma\gamma}, \tilde{A}_{ZZ}, \tilde{A}_{\gamma Z}, \tilde{A}_{Z\gamma}$ belong. In our notations $A_{\gamma\gamma}^{(Box)}$ is the component of the scattering amplitude at one loop that appears in the form $v_{\mu,e}^{(\gamma)} A_{\gamma\gamma}^{(Box)} v_f^{(\gamma),\mu}$ where $v_{e,f}^{(\gamma),\mu} \equiv -|e_0| Q_{e,f} \gamma^\mu$ is what we call the photon Lorentz structure and analogous definitions are obtained for $A_{ZZ}^{(Box)}, A_{\gamma Z}^{(Box)}, A_{Z\gamma}^{(Box)}$ with the Z Lorentz structure defined as $v_{e,f}^{(Z),\mu} \equiv -\frac{|e_0|}{2s_0 c_0} \gamma^\mu (g_{V,e,f}^0 - g_{A,e,f}^0 \gamma^5)$. We do not insist here on these technical points that are, we repeat, fully discussed in previous references [8–11]. Our notations are almost rigorously following the conventions of Degrassi and Sirlin [12,13], and our approach is often motivated by their previous observations. In particular, one can immediately understand that all the four quantities listed in Eqs. (2.1)-(2.4) are separately gauge-independent, since they contribute different Lorentz structures of the process. As a consequence of this fact, whenever computing contributions e.g. from virtual W s exchanges, that are intrinsically gauge dependent, it will be essential for a clean interpretation of the result to stick the various effects in the proper previous combinations.

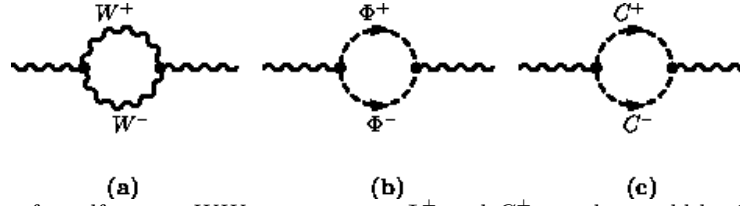


FIG. 1. Feynman diagrams for self-energy WW components. Φ^\pm and C^\pm are the would-be Goldstone bosons and ghosts, respectively.

To illustrate the previous qualitative statements with a concrete example, we start from the calculation of the charged boson contributions to the generalized photonic correction $\tilde{\Delta}_{\alpha,ef}(q^2, \theta)$ of Eq. (2.1). Since this quantity is by construction gauge-independent, we have performed the calculation in the familiar t'Hooft gauge. This means that the contributions from the unphysical charged would-be Goldstone bosons must be incorporated and added to those coming from the charged W s (and ghosts). We shall follow the order given by the various definitions and compute the transverse self-energies terms first. In the case of $\tilde{\Delta}_{\alpha,ef}$, these correspond to the Feynman diagrams shown in Fig. 1. A straightforward calculation leads to the result (only the sum of all separate terms of Fig. 1 is given):

$$\begin{aligned} \tilde{\Delta}_{\alpha,e\mu}^{s.e. (WW)}(q^2) &= F_{\gamma\gamma}^{1a+1b+1c}(0) - F_{\gamma\gamma}^{1a+1b+1c}(q^2) = \\ &= -\left(\frac{5\alpha}{4\pi}\right) \left\{ \int_0^1 dx \left[1 - \frac{12}{5}x(1-x) \right] \ln \left| 1 - \frac{q^2}{M_W^2}x(1-x) \right| \right. \\ &\quad \left. + \frac{4}{15} + \frac{8M_W^2}{5q^2} \int_0^1 dx \ln \left| 1 - \frac{q^2}{M_W^2}x(1-x) \right| \right\} \end{aligned} \quad (2.11)$$

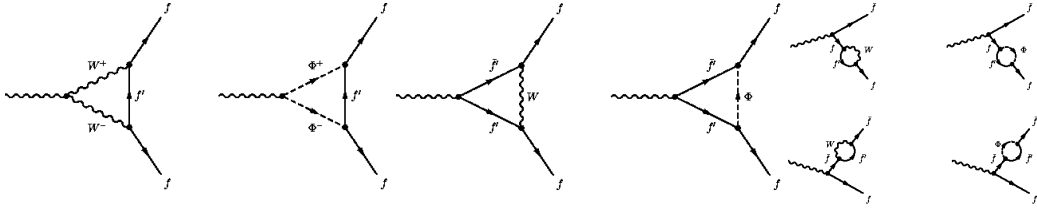


FIG. 2. Feynman diagrams for WW vertex component (Fig. 2a), for single W vertex (Fig. 2b) and for fermion self-energy diagrams (Fig. 2c).

The previous self-energy component $\tilde{\Delta}_{\alpha,ef}^{s.e. (WW)}$ is universal i.e. independent of the final fermion features. This is not true for the remaining vertex and box contributions. It is convenient therefore to consider the various cases separately by treating final muons (or taus), final u quarks and final d quarks states in succession. Starting with final muons, we have first to consider the diagram involving W s in Fig. 2a (we are assuming massless final fermions, so that their couplings with would-be Goldstone Φ bosons vanish). There is also no photon-neutrino coupling so no diagram of the type of Fig. 2b. In principle one should finally add the fermion self-energy diagrams of Fig. 2c. However their contribution is q^2 -independent and disappears in the subtraction. This is also the case for any type of tadpole diagram, that we therefore never discuss here. This leads to the following expression of the (two W s) contribution to the generalized vertex $\Gamma_{\mu,\gamma}(q^2)$, to be conventionally defined as $\Gamma_{\mu,\gamma}^{(WW)}(q^2)$:

$$\Gamma_{\mu,\gamma}^{(WW)(2a+2b)}(q^2) = -\left(\frac{e^3}{64\pi^2 s^2}\right) \gamma_\mu (1 - \gamma^5) \left\{ -2\left(\frac{1}{\epsilon} - \bar{\gamma}\right) + \frac{3}{2} - \ln M_W^2 \right. \\ \left. + 2 \iint dx_1 dx_2 \left[3 \ln |M_W^2(x_1 + x_2) - q^2 x_1 x_2| + \frac{q^2(x_1 + x_2 - x_1 x_2)}{M_W^2(x_1 + x_2) - q^2 x_1 x_2} \right] \right\} \quad (2.12)$$

where $\epsilon = (4 - n)/2$ and $\bar{\gamma} = \ln(4\pi) + \gamma$, γ being the Euler-Mascheroni constant.

Projecting this vertex on the photon Lorentz structure, according to our procedure, gives then

$$\tilde{\Delta}_{\alpha,e\mu}^{vert. (WW)}(q^2) = -\left(\frac{\alpha}{\pi}\right) \iint dx_1 dx_2 \left[3 \ln \left| 1 - \frac{q^2 x_1 x_2}{M_W^2(x_1 + x_2)} \right| + \frac{q^2(x_1 + x_2 - x_1 x_2)}{M_W^2(x_1 + x_2) - q^2 x_1 x_2} \right] \quad (2.13)$$

For a final $u\bar{u}$ or $d\bar{d}$ pair, we have to include in the calculation of $\Gamma_{\mu,\gamma}(q^2)$ another (single W) diagram as shown in Fig. 2b. This is, in fact, the non universal component of such charged boson vertex, since to the graph of Fig. 2a with two W s a universal quantity is associated. Strictly speaking, diagrams with charged would-be Goldstone bosons should also be included when the mass of the involved quarks cannot be neglected. This corresponds to the cases of final $t\bar{t}$ pairs and of final $b\bar{b}$ pairs. Top production will not be considered in this paper since our technique, based on Z peak subtraction, does not apply in this case; for $b\bar{b}$ final states the specific calculation of that contribution to the vertex will be given in Sec. A 1. For “light” u, d quarks we then obtain the following contributions (we give the projection on the $\tilde{\Delta}_{\alpha,ef}(q^2, \theta)$ combination directly):

$$\tilde{\Delta}_{\alpha,eu}^{vert. (W)}(q^2) = \frac{\alpha}{6\pi} \iint dx_1 dx_2 \left[\ln \left| 1 - \frac{q^2 x_1 x_2}{M_W^2(1 - x_1 - x_2)} \right| - \frac{q^2(1 - x_1)(1 - x_2)}{M_W^2(1 - x_1 - x_2) - q^2 x_1 x_2} \right] \quad (2.14)$$

$$\tilde{\Delta}_{\alpha,ed}^{vert. (W)}(q^2) = 2\tilde{\Delta}_{\alpha,eu}^{vert. (W)}(q^2) \quad (2.15)$$

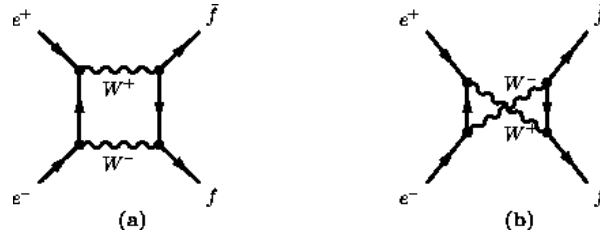


FIG. 3. Feynman diagrams for WW box contribution; $I_{3f} = -\frac{1}{2}$ (Fig. 3a), $I_{3f} = +\frac{1}{2}$ (Fig. 3b).

The final step is now the addition of the box contributions, that correspond to the single Feynman diagram of Fig. 3 ((a) for final states with $I_{3f} = -\frac{1}{2}$, (b) for $I_{3f} = +\frac{1}{2}$) in the cases where the mass of the final quarks can be neglected (in practice, for our purposes, the only exception would be the box with a final $b\bar{b}$ pair, to be discussed in the appendix together with the related vertex). The expression of the WW box contribution to the full scattering amplitude has been already given in the literature [14]. By a straightforward projection on the photon Lorentz structures one easily obtains for final $\mu^+\mu^-$, $u\bar{u}$, $d\bar{d}$ pairs

$$\tilde{\Delta}_{\alpha,e\mu}^{Box (WW)}(q^2, \theta) = \frac{\alpha}{32\pi s^4}(1 - v_e)^2[I(q^2, t, M_W) + I_5(q^2, t, M_W)] \quad (2.16)$$

$$\tilde{\Delta}_{\alpha,eu}^{Box (WW)}(q^2, \theta) = \frac{3\alpha}{64\pi s^4}(1 - v_e)(1 - v_u)[I(q^2, u, M_W) - I_5(q^2, u, M_W)] \quad (2.17)$$

$$\tilde{\Delta}_{\alpha,ed}^{Box (WW)}(q^2, \theta) = \frac{3\alpha}{32\pi s^4}(1 - v_e)(1 - v_d)[I(q^2, t, M_W) + I_5(q^2, t, M_W)] \quad (2.18)$$

where $v_f \equiv 1 - 4|Q_f|s^2$ and $I(q^2, t, M_W)$, $I_5(q^2, t, M_W)$, $I(q^2, u, M_W)$, $I_5(q^2, u, M_W)$ are known functions ¹ defined in Sec. A 3, with $t = -\frac{q^2}{2}(1 - \cos\theta)$, $u = -\frac{q^2}{2}(1 + \cos\theta)$.

The full charged boson contribution is then given by the sum:

$$\tilde{\Delta}_{\alpha,ef}^{(charged W)}(q^2, \theta) = \tilde{\Delta}_{\alpha,ef}^{s.e. (WW)}(q^2) + \tilde{\Delta}_{\alpha,ef}^{vert. (WW)}(q^2) + \tilde{\Delta}_{\alpha,ef}^{vert. (W)}(q^2) + \tilde{\Delta}_{\alpha,ef}^{Box (WW)}(q^2, \theta) \quad (2.19)$$

in which the self-energy component is universal, the vertex with two Ws is also universal except for the m_t^2 dependent terms for $b\bar{b}$ final states and the vertex with one W and the box terms depend on the final state.

The calculation of the charged boson contribution to the three remaining gauge independent combinations R , $V^{\gamma Z}$, $V^{Z\gamma}$ proceeds now in strict analogy with that illustrated for $\tilde{\Delta}_{\alpha,ef}$, replacing the initial photon with an initial Z . The calculations are straightforward and do not require a special mention. Rather than illustrating them in detail with a long series of formulae, we just refer to Secs. A 1 and A 3 in which all the individual terms of the following sums are given:

$$R_{ef}^{(charged W)}(q^2, \theta) = R_{ef}^{s.e. (WW)}(q^2) + R_{ef}^{vert. (WW)}(q^2) + R_{ef}^{vert. (W)}(q^2) + R_{ef}^{Box (WW)}(q^2, \theta) \quad (2.20)$$

$$V_{ef}^{\gamma Z (charged W)}(q^2, \theta) = V_{ef}^{s.e. (WW)}(q^2) + V_{ef}^{\gamma Z, vert. (WW)}(q^2) + V_{ef}^{\gamma Z, vert. (W)}(q^2) + V_{ef}^{\gamma Z, Box (WW)}(q^2, \theta) \quad (2.21)$$

$$V_{ef}^{Z\gamma (charged W)}(q^2, \theta) = V_{ef}^{s.e. (WW)}(q^2) + V_{ef}^{Z\gamma, vert. (WW)}(q^2) + V_{ef}^{Z\gamma, vert. (W)}(q^2) + V_{ef}^{Z\gamma, Box (WW)}(q^2, \theta) \quad (2.22)$$

From the previous expressions Eqs. (2.19)-(2.22), we are now in a position to derive the charged boson contribution to any observable of the process $e^+e^- \rightarrow f\bar{f}$ ($f \neq e$). This is made possible by the expression that the related differential cross section assumes in our formalism. We shall be limited for the moment to the situation where polarized electron beams are not considered (this might be a very interesting case in future measurements, as stressed in a previous paper [15]). In this case, we shall write:

$$\frac{d\sigma_{ef}}{d\cos\theta}(q^2, \theta) = \frac{3}{8}(1 + \cos^2\theta)\sigma_1^{ef} + \cos\theta\sigma_2^{ef} \quad (2.23)$$

where

¹ We thank W. Hollik for sending us his Fortran implementation of these functions.

$$\begin{aligned}
\sigma_1^{ef} = & N_f(q^2) \left(\frac{4\pi q^2}{3} \right) \left\{ \frac{\alpha^2(0) Q_f^2}{q^4} [1 + 2\tilde{\Delta}_{\alpha,ef}(q^2, \theta)] \right. \\
& + 2\alpha(0) |Q_f| \left[\frac{q^2 - M_Z^2}{q^2((q^2 - M_Z^2)^2 + M_Z^2 \Gamma_Z^2)} \right] \left[\frac{3\Gamma_e}{M_Z} \right]^{1/2} \left[\frac{3\Gamma_f}{N_f(M_Z^2) M_Z} \right]^{1/2} \frac{\tilde{v}_e \tilde{v}_f}{(1 + \tilde{v}_e^2)^{1/2} (1 + \tilde{v}_f^2)^{1/2}} \\
& \times [1 + \tilde{\Delta}_{\alpha,ef}(q^2, \theta) - R_{ef}(q^2, \theta) - 4s_e c_e \left\{ \frac{1}{\tilde{v}_e} V_{ef}^{\gamma Z}(q^2, \theta) + \frac{|Q_f|}{\tilde{v}_f} V_{ef}^{Z\gamma}(q^2, \theta) \right\}] \\
& + \frac{\left[\frac{3\Gamma_e}{M_Z} \right] \left[\frac{3\Gamma_f}{N_f(M_Z^2) M_Z} \right]}{(q^2 - M_Z^2)^2 + M_Z^2 \Gamma_Z^2} [1 - 2R_{ef}(q^2, \theta) - 8s_e c_e \left\{ \frac{\tilde{v}_e}{1 + \tilde{v}_e^2} V_{ef}^{\gamma Z}(q^2, \theta) + \frac{\tilde{v}_f |Q_f|}{(1 + \tilde{v}_f^2)} V_{ef}^{Z\gamma}(q^2, \theta) \right\}] \left. \right\}
\end{aligned} \tag{2.24}$$

$$\begin{aligned}
\sigma_2^{ef} = & \frac{3N_f(q^2)}{4} \left(\frac{4\pi q^2}{3} \right) \left\{ 2\alpha(0) |Q_f| \left[\frac{(q^2 - M_Z^2)}{q^2((q^2 - M_Z^2)^2 + M_Z^2 \Gamma_Z^2)} \right] \left[\frac{3\Gamma_e}{M_Z} \right]^{1/2} \left[\frac{3\Gamma_f}{N_f(M_Z^2) M_Z} \right]^{1/2} \right. \\
& \times \frac{1}{(1 + \tilde{v}_e^2)^{1/2} (1 + \tilde{v}_f^2)^{1/2}} [1 + \tilde{\Delta}_{\alpha,ef}(q^2, \theta) - R_{ef}(q^2, \theta)] + \frac{\left[\frac{3\Gamma_e}{M_Z} \right] \left[\frac{3\Gamma_f}{N_f(M_Z^2) M_Z} \right]}{(q^2 - M_Z^2)^2 + M_Z^2 \Gamma_Z^2} \\
& \times \left[\frac{4\tilde{v}_e \tilde{v}_f}{(1 + \tilde{v}_e^2)(1 + \tilde{v}_f^2)} \right] [1 - 2R_{ef}(q^2, \theta) - 4s_e c_e \left\{ \frac{1}{\tilde{v}_e} V_{ef}^{\gamma Z}(q^2, \theta) + \frac{|Q_f|}{\tilde{v}_f} V_{ef}^{Z\gamma}(q^2, \theta) \right\}] \left. \right\}
\end{aligned} \tag{2.25}$$

where $N_f(q^2)$ is the conventional color factor which contains standard QCD corrections at variable q^2 and the theoretical input of Eqs. (2.24),(2.25) contains Γ_e , Γ_f , $\tilde{v}_e \equiv 1 - 4s_e^2$, $\tilde{v}_f \equiv 1 - 4|Q_f|s_f^2$ measured on top of Z resonance with an accuracy that is sufficient to prevent any dangerous theoretical uncertainty in our predictions for future e^+e^- colliders, given their expected realistic experimental accuracy, as exhaustively discussed in Refs. [8,9].

From the previous Eqs. (2.19)-(2.22) it is now perfectly clear how to compute, in a rigorously gauge-independent way, the charged W contribution to various observables. This is the result of the insertion in those equations of the charged boson contributions that we have listed.

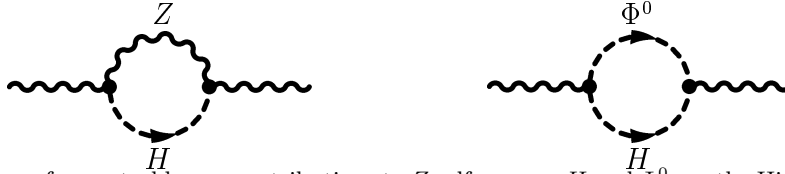


FIG. 4. Feynman diagrams for neutral boson contributions to Z self-energy. H and Φ^0 are the Higgs boson and the would-be Goldstone boson, respectively.

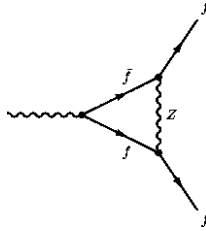


FIG. 5. Feynman diagram for Z vertex insertion.

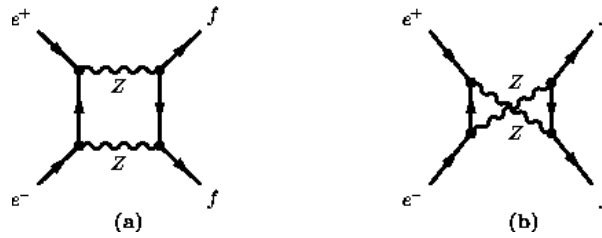


FIG. 6. Feynman diagrams for ZZ box contribution.

In a quite analogous way, one would compute the overall neutral boson component or the fermionic contribution to only self-energies, that is separately gauge independent. In fact, we have also evaluated the neutral boson contribution by an analogous calculation, involving Z self-energies (Fig. 4), Z vertices (Fig. 5) and ZZ boxes (Fig. 6) (including when necessary the neutral would-be Goldstone bosons and Higgs exchanges). Without entering the details of the procedure, we anticipate that these terms contribute, for reasonable values of the Higgs mass, all observables by an amount that is much smaller than that coming from the charged boson diagrams. The light fermion self-energy contribution (Fig. 7) is, on the contrary, relevant and must be suitably taken into account for a complete numerical estimate. This will be discussed in detail in the two forthcoming Sections.

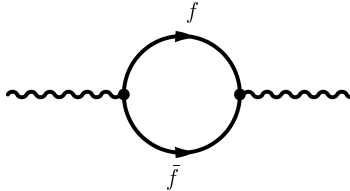


FIG. 7. Feynman diagram for fermionic contribution to self-energy correction.

III. PREDICTIONS FOR OBSERVABLES IN ABSENCE OF PHOTON EMISSION

Our final step has been at this point that of translating all the previously illustrated calculations into realistic numerical predictions for the various observables of the process $e^+e^- \rightarrow ff$. We have concentrated our attention in an energy range $\sqrt{q^2}$ between the Z resonance and 1 TeV, although we could have considered higher energies as well. Technically speaking, we have divided our programs into two separate phases. In the first one, we have written analytic expressions for the four quantities $\tilde{\Delta}_\alpha$, R , $V^{\gamma Z}$, $V^{Z\gamma}$ that should contain the bulk of the numerically relevant components (we have systematically ignored, as one might have noticed, imaginary parts in the various quantities; this approximation should be quite tolerable at high energies). More precisely, we have taken into account in a conventional way, i.e. including leading-log resummation, the running of α_{QED} , due to fermion loops, that appears in $\tilde{\Delta}_\alpha$ (and plays a fundamental role)² and we have also inserted the full fermion contribution to the Z and γZ self-energies. These terms, added to the leading terms that contain α , M_Z and the Z -peak quantities, will constitute what we shall call “non bosonic component” of the various observables. To these expressions we have added those given in Eqs. (2.19)-(2.22), plus the negligible neutral boson component. These terms will generate the charged and neutral boson contributions to all observables.

The second phase of our approach has been that of implementing our theoretical expressions into a semi-analytical program called PALM (PAViaLecceMontpellier program). This program, which is already available, will be fully illustrated in a separate dedicated publication. In PALM all the integrations over the Feynman variables yielding the one loop subtracted self-energy and vertex corrections are performed numerically [16] according to semi-analytical algorithms optimized to guarantee reliable and accurate results for the electroweak effects. In particular, the two-dimensional integrals providing the vertex contributions are first analytically reduced to one-dimensional integrals,

²The leptonic contribution to α_{QED} is exactly included as well as the top-quark effect, both below and above the $t\bar{t}$ threshold. The light quark contribution has been implemented following the generally adopted parameterization of Eidelman-Jegerlehner in Ref. [2].

that are then treated numerically on the same ground as the self-energy corrections. A numerical integration over the fermion scattering angle is performed for weak boxes in order to get their contribution to the integrated cross section and forward-backward asymmetry. It has been checked that the numerical procedure adopted provides results in perfect agreement with the formulae obtained by analytic integration over the Feynman parameters. The complete one loop electroweak contributions to $\tilde{\Delta}_{\alpha,ef}$, R_{ef} , $V_{ef}^{\gamma Z}$ and $V_{ef}^{Z\gamma}$ are codified in PALM following a completely modular structure, where the corrections contributing each Lorentz structure are grouped into a single routine. This will allow a quite easy implementation in the program of analogous virtual effects, such those due to SUSY and other new physics models.

To check the validity of our computation we have first compared our numerical results, without taking QED radiation into account, with the corresponding ones of the most recent version of the program TOPAZ0 [17]. The input parameters used for the comparison are $M_Z = 91.1867$ GeV, $m_{top} = 160$ GeV, $m_{Higgs} = 115$ GeV and $\alpha_s(M_Z) = 0.120$, together with the most recent data for Z peak observables needed as input in PALM [18]. For the sake of comparison, the value $m_{top} = 160$ GeV has been chosen because fits to all electroweak data except the direct determination of m_{top} and M_W prefer a “low” top mass [18] and therefore this choice turns out to be consistent with the input Z peak observables of PALM. Further, for a meaningful comparison with the TOPAZ0 predictions, the input Z partial widths of PALM have been corrected for the effect of standard QED final-state correction. For simplicity we have not included at this level in our program the aforementioned heavy top contributions to the b vertex and box. These actually only contribute the $b\bar{b}$ differential cross section, and will affect the total hadronic quantities that we have considered (in practice, at this preliminary stage, the cross section for production of the five light u, d, s, c, b quarks) to a presumably negligible extent (we shall return to this point later on).

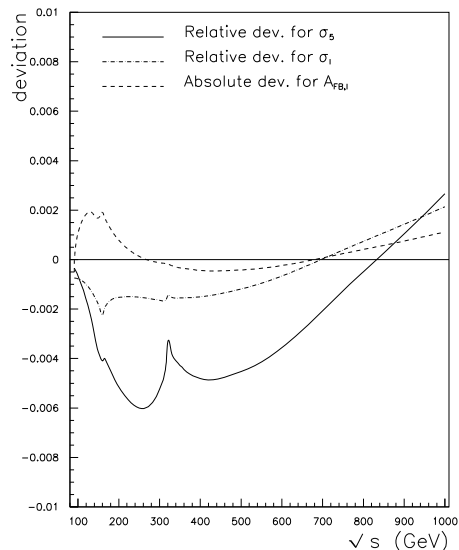


FIG. 8. Comparison between the predictions of PALM and those of TOPAZ0 for the leptonic and hadronic cross section σ_l ($l \neq e$) and σ_5 (relative deviations) and for the leptonic forward-backward asymmetry $A_{FB,l}$ (absolute deviation).

The comparison has been carried through in an energy range $\sqrt{q^2}$ between M_Z and 1 TeV. It is depicted graphically in Fig. 8 for three observables, chosen on the basis of their expected good experimental accuracy: the cross section σ_l for production of charged leptons ($l \neq e$), the related forward-backward asymmetry $A_{FB,l}$ and the cross section for five light quark production σ_5 .

As one sees from Fig. 8, the agreement between our calculations and those of TOPAZ0 is indeed impressive in the full considered energy range. This is particularly true for the two leptonic observables, for which the difference between the two approaches is always less than about two permille, well below the expected experimental accuracy, estimated to be of about a relative one percent [19]. This is also true for the hadronic cross section, with the exception of two small regions around 300 GeV and at the end of the range when $\sqrt{q^2}$ approaches 1 TeV, where the relative difference reaches a five per mille value that is, though, still below the one percent expected experimental accuracy. In fact, we believe that this discrepancy can be originated by the heavy top effect in the b vertex and box that we did not include in our program, and are contained in TOPAZ0. Since this difference is indeed modest, we feel that it can be safely neglected at this stage. Note that we did not consider the intrinsic theoretical errors implicitly contained

in both programs (e.g. PALM has as theoretical input a number of Z widths and asymmetries). We estimated such uncertainties to be, typically, of the permille size in both cases, which would still reduce the (already miserable) existing discrepancy.

Having checked in this way the reliability of our calculation, we now move to the real goal of this paper, that is the consideration of the (charged) boson effects. These are shown for the three separate variables σ_μ , $A_{FB,\mu}$ and σ_5 in Fig. 9 as computed by our program PALM.

As one clearly sees from Fig. 9 the effect of such bosonic contributions becomes indeed relevant as soon as the c.m. energy raises above a typical value of approximately 200 GeV, that corresponds to the LEP2 limit. At energies of about 500 GeV, in the expected range of a future e^+e^- linear collider (LC) [6], the relative size of the bosonic terms is already larger than two percent in σ_μ and six percent in σ_5 . This relative effect continues to rise when the c.m. energy increases, reaching values of the ten percent size in the hadronic cross section in the 1 TeV limit. This clearly generates, in our opinion, two independent and rather relevant theoretical issues.

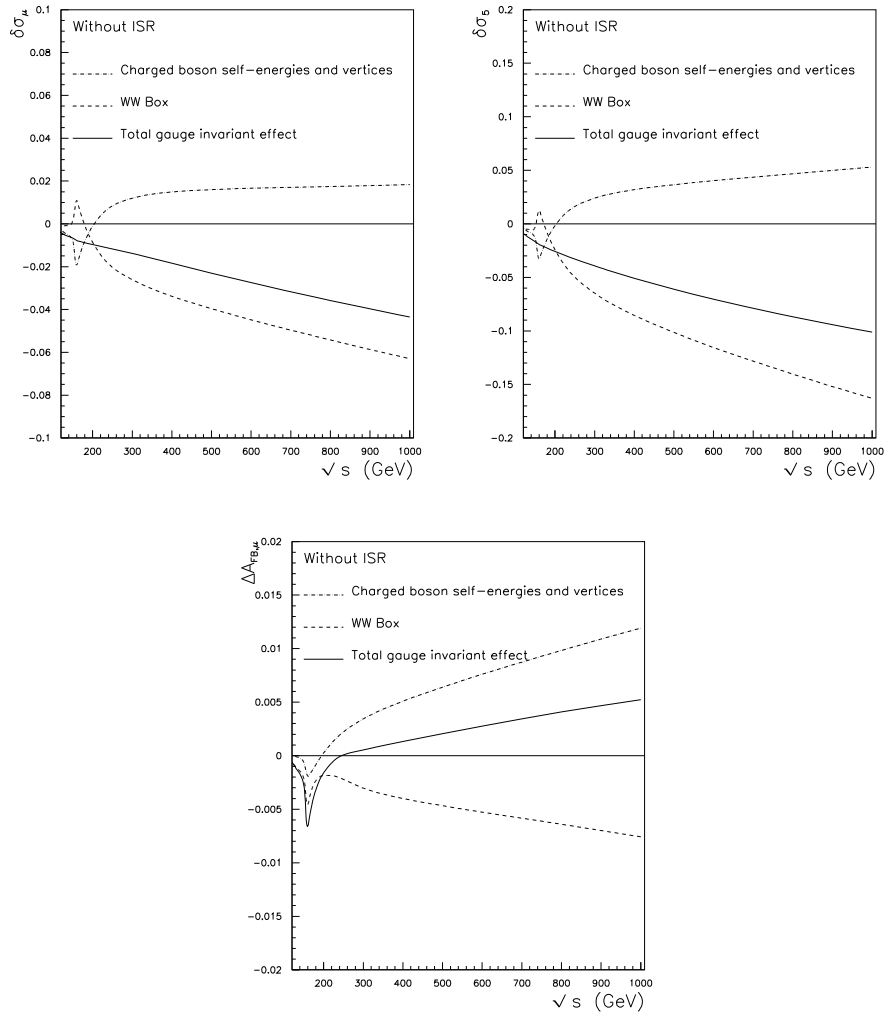


FIG. 9. The rising charged boson effects as functions of the c.m. energy, for the three observables σ_μ , σ_5 and $A_{FB,\mu}$, in absence of photon emission. The separate effect of charged boson self-energies and vertices (dash-dotted line), WW box (dashed line) and their gauge invariant sum (solid line) is plotted. The relative effect of charged boson effects is shown with respect to the observables including the gauge independent overall neutral boson component and fermionic corrections.

The first problem is that of understanding the reasons of such a visible rise. At first sight, this appears to be stronger than a purely logarithmic one, as it can be easily checked by numerical inspection. Should this be indeed the case, one could not advocate the expected asymptotic purely logarithmic increase dictated by renormalization group arguments that would apply to the transverse self-energies (in their generalized gauge independent definition proposed

in Refs. [12,13], that also includes a small amount of “pinched” vertex [20]). The extra increase should therefore be rather addressed to the remaining component of the various combinations (by this we mean what would remain after the purely logarithmic, separately gauge independent, “generalized” Degrassi-Sirlin self-energies have been isolated).

As a matter of fact, it has been pointed out in a previous reference [21], and stressed again in Ref. [12], that the non pinch part of the W vertex, Fig. 2b, behaves in the large q^2 limit as the squared logarithm of q^2/M_W^2 . Such a behaviour is often denoted as a “Sudakov logarithm” [22] since the limit $q^2/M_W^2 \rightarrow \infty$, is formally identical to an “infrared”, QED like, $M_W \rightarrow 0$ limit. On general QED analogy arguments, one would expect such terms to appear also in the box contributions to the various combinations. More practically, one actually sees such terms in the analytic expressions of boxes given in Sec. A 3. Thus, the existence of such a behaviour at large q^2 appears to us theoretically expected.

Strictly related with this increase is, in our opinion, the problem of how to treat perturbatively such effects when they become too large. In other words, one should study a mechanism of resummation analogous to that proposed by Sudakov [22] in the QED case. Although this problem is at the moment of rather academic interest (since after all even at 1 TeV the effect is still below ten percent), it might become rather relevant in the case of future colliders at energies in the few TeV range.

The second problem that arises is a consequence of the fact that the bosonic effect is, in any case, sizeable when one moves beyond the LEP2 energy limit. This means that a proper estimate of photon emission effects, that also includes such full bosonic terms in the quantities to be convoluted, becomes imperative. We shall perform this calculation in the next Sec. IV. This will require a technical discussion which we tried to make as concise as possible.

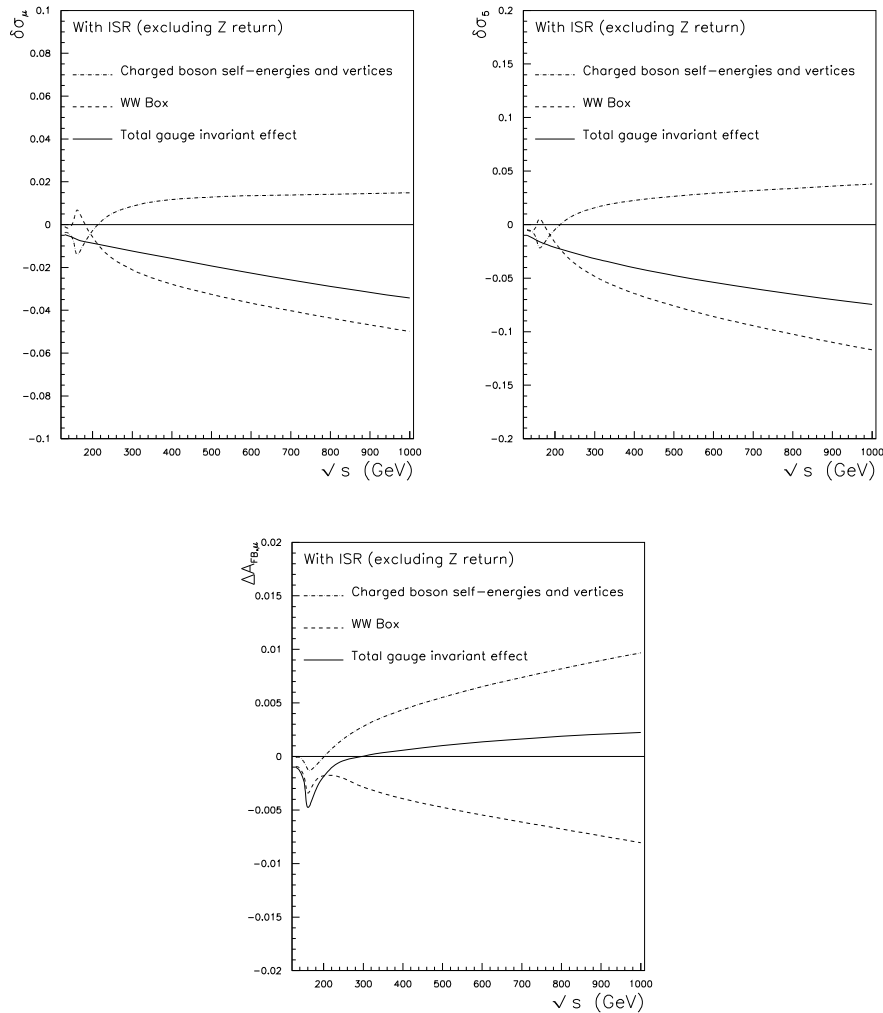


FIG. 10. The same as Fig. 9, including QED initial-state radiation (ISR). The cut $\sqrt{s'} > 100$ GeV, s' being the invariant mass of the event after ISR, is imposed to exclude the Z radiative return.

IV. TREATMENT OF PHOTON EMISSION EFFECTS

For the aim of the present study, we are interested in the contribution of the initial-state radiation (ISR), since it is well known that it constitutes the largely dominating QED effect.³ The evaluation of QED radiation effects has been obtained in our calculation adopting the QED Structure Function (SF) method [7]. It provides a simple, non-perturbative approach, based on factorization theorems of infrared and collinear singularities, for computing leading-log (LL) photonic corrections to any arbitrary e^+e^- hard-scattering cross section. The method allows to keep under control the long-distance universal logarithmic contributions, due to the soft and/or collinear photon radiation, by convoluting a kernel cross section with electron(positron) structure functions. For a typical event selection where a cut on the invariant mass of the event after ISR is imposed, the QED corrected cross section can be simply calculated as [7,23]

$$\sigma(s) = \int_0^{1-x_{cut}} dx H(x, s) \sigma_0((1-x)s) \quad (4.1)$$

where $H(x, s)$ is the radiator or flux function, and σ_0 is the elementary de-convoluted cross section eventually including, as in our case, the process-dependent pure weak and QCD corrections. The radiator represents the probability that a fraction x of the whole c.m. energy s is carried away by ISR and is calculable as:

$$H(x, s) = \int_{1-x}^1 \frac{dz}{z} D(z, s) D\left(\frac{1-x}{z}s\right) \quad (4.2)$$

where $D(x, s)$ is the electron SF. A typical solution for the radiator, generally used for LEP1/SLC calculations, reads [7,23]:

$$\begin{aligned} H(x, s) &= \Delta_2 \beta x^{\beta-1} + h_1(x, s) + h_2(x, s) \\ h_1(x, s) &= -\frac{1}{2}\beta(2-x) \\ h_2(x, s) &= \frac{1}{8}\beta^2 \left[(2-x)(3\ln(1-x) - 4\ln x) - 4\frac{\ln(1-x)}{x} + x - 6 \right] \\ \beta &= 2\left(\frac{\alpha}{\pi}\right) [L - 1], \quad L = \ln(s/m^2), \quad \Delta_2 = 1 + \left(\frac{\alpha}{\pi}\right) \delta_1 + \left(\frac{\alpha}{\pi}\right)^2 \delta_2. \end{aligned} \quad (4.3)$$

The first exponentiated term in $H(x, s)$ describes all order soft multi-photon emission, $h_{1,2}(x, s)$ are associated to hard bremsstrahlung in collinear approximation, β being the QED collinear factor. The perturbative coefficient Δ_2 is the $\mathcal{O}(\alpha^2)$ soft+virtual K factor for s -channel processes. Equation (4.3) for the QED radiator, that accurately works for precision studies of the electroweak interactions on top of the Z resonance, becomes inadequate far from it, where, as discussed in Ref. [24], higher-order hard photon effects may become numerically relevant as a consequence of the phenomenon of Z radiative return. Actually, as pointed out in Ref. [24], $\mathcal{O}(\alpha^2)$ next-to-leading (NL) hard-photon corrections, that are known from the exact $\mathcal{O}(\alpha^2)$ diagrammatic calculation [25] and numerically negligible close to the Z peak, introduce measurable effects at LEP2 and beyond and can be taken into account with the replacement

$$H(x, s) \rightarrow H(x, s) - h_2(x, s) + \delta_2^H(1-x, s) \quad (4.4)$$

where the explicit expression for δ_2^H can be found in Ref. [26]. These $\mathcal{O}(\alpha^2 L)$ corrections are of the same order of magnitude as the third-order LL ones, that come from the emission of three hard collinear photons and have been recently analyzed in the literature for their impact on two-fermion production cross sections at LEP2 [24]. Including both NL $\mathcal{O}(\alpha^2)$ and LL $\mathcal{O}(\beta^3)$ contributions, an accurate QED radiator in analytic form can be cast as follows [24]:

³In principle, one should also consider other conventional QED effects as those due to final-state radiation and initial-final state interference. However, for the experimental set up considered in the following, the (very small) effect of final-state radiation is automatically included in our approach by means of the input physical quantities Γ_f . Further, the contribution of initial-final state interference and QED boxes has been evaluated by using the previously quoted program TOPAZ0 and found to be negligible as compared to the effect of ISR.

$$\begin{aligned}
H(x, s) &= \Delta_3 \beta x^{\beta-1} + h_1(x, s) + \delta_2^H(1-x, s) + h_3(x, s) \\
h_3(x, s) &= \frac{1}{3!} \left(\frac{\beta}{2}\right)^3 \left[-\frac{27}{2} + \frac{15}{4}x + 4\left(1 - \frac{1}{2}x\right) (\pi^2 - 6 \ln^2 x + 3\text{Li}_2(x)) \right. \\
&\quad \left. + 3 \ln(1-x) \left(7 - \frac{6}{x} - \frac{3}{2}x\right) + \ln^2(1-x) \left(-7 + \frac{4}{x} + \frac{7}{2}x\right) \right. \\
&\quad \left. - 6 \ln x(6-x) + 6 \ln x \ln(1-x) \left(6 - \frac{4}{x} - 3x\right) \right] \\
\Delta_3 &= \Delta_2 + \left(\frac{\alpha}{\pi}\right)^3 \delta_3 \\
\delta_3 &= (L-1)^3 \left(\frac{9}{16} - \frac{1}{2}\pi^2 - \frac{4}{3}\psi^{(2)}(1)\right)
\end{aligned} \tag{4.5}$$

where $\psi^{(n)}(z)$ is the n -th order polygamma function, $\psi^{(n)}(z) = d^n \psi(z)/dz^n$, $\psi(z) = \Gamma'(z)/\Gamma(z)$. Equation (4.1), together with the radiator of Eq. (4.5), is the formulation implemented in PALM for the simulation of initial-state photonic effects to the muon and hadronic cross section.

Since the numerator of the forward-backward asymmetry is a less inclusive quantity than a fully integrated cross section, the convolution integral for the asymmetry is different from that of the total cross section and is given by [27]

$$A_{FB}(s) = \frac{1}{\sigma(s)} \int_0^{1-x_{cut}} dx \frac{4(1-x)}{(2-x)^2} H_{FB}(x, s) \sigma_{FB}((1-x)s) \tag{4.6}$$

where $\sigma_{FB}(s)$ is the forward minus backward cross section and $\sigma(s)$ is the total cross section as given by Eq. (4.1). The radiator $H_{FB}(x, s)$ can be written as

$$H_{FB}(x, s) = H(x, s) + h_{FB,1}^{NL}(x, s) + h_{FB,2}^{LL}(x, s) \tag{4.7}$$

where $H(x, s)$ is the radiator of Eq. (4.3), $h_{FB,1}^{NL}$ stands for $\mathcal{O}(\alpha)$ NL corrections to s -channel processes [28], $h_{FB,2}^{LL}$ are $\mathcal{O}(\alpha^2)$ LL ‘‘antisymmetric’’ corrections [29]. Equation (4.6), with the radiator of Eq. (4.7), is the convolution integral implemented in PALM for the calculation of QED radiation effects to the muon asymmetry.

In the program PALM the integrations of Eqs. (4.1) and (4.6) are performed numerically by using a semi-analytical procedure improved by standard importance sampling tricks to take care of the infrared and Z radiative return peaking behaviour.

The impact of the initial-state photon emission on rising electroweak virtual effects is shown in Fig. 10 and Fig. 11, for two different typically adopted selection criteria, i.e. excluding the Z return ($\sqrt{s'} > 100$ GeV, with $s' = (1-x)s$) and including it ($\sqrt{s'} > 20$ GeV). As it can be clearly seen, a proper inclusion of QED radiation is unavoidable to get a reliable evaluation of bosonic virtual effects. Actually, when excluding the Z return, the QED convolution can give a relative reduction of the order of 25-30% of the overall bosonic effects to σ_μ and σ_5 and a significant lowering of the same effects to $A_{FB,\mu}$. When including the Z return, the impact of the QED convolution is much larger, reaching a 60-80% relative effect in the cross sections and changing sign to the net effect to the forward-backward asymmetry. The event selection with the inclusion of Z return, in particular, is responsible of a much flatter behaviour of the bosonic corrections, whereas the exclusion of Z radiative return reduces the absolute size of the corrections without critically modifying their peculiar rising slope. Typically, the size of the effect on the hadronic cross section at 500 GeV is reduced by QED convolution from six percent to four percent, which certainly represents a drastic difference visible at an expected experimental accuracy below the 1% level.

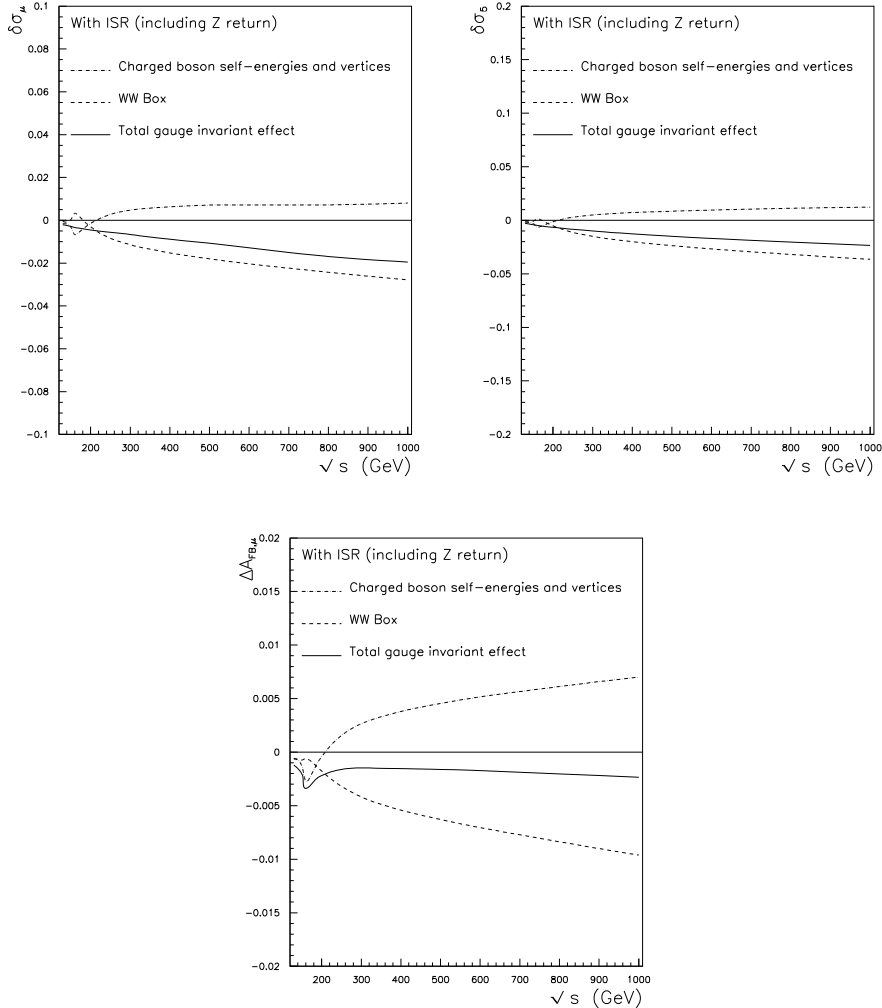


FIG. 11. The same as Fig. 10, with $\sqrt{s'} > 20$ GeV, to include the Z radiative return.

V. CONCLUDING REMARKS

We have shown in this paper that an accurate computation of theoretical predictions for the process of e^+e^- annihilation into charged fermion pairs at future high energy colliders requires the full determination of the bosonic contributions, including boxes which are usually neglected on top of the Z resonance. We have performed the relevant calculations in the t' Hooft gauge, but the overall contributions that we have shown are completely gauge-independent. For this overall effect we conclude that, since the contribution from its “generalized” gauge independent self-energies can only be of logarithmic type when q^2 becomes large, extra stronger effects of Sudakov type can only be produced by the combination of the “non pinched” parts of vertices with the boxes. These rising effects are evident in our calculation, and become visible as soon as one crosses the 200 GeV range. As we have shown, the effect of a proper inclusion of QED radiation is indeed numerically essential and should be carefully taken into account in the theoretical predictions.

One possible interesting generalization of our investigation would be the search for analogous sizeable contributions in a SUSY calculation of virtual effects at future colliders. On a qualitative basis, we would expect the presence of important effects produced by either chargino or even neutralino vertices and boxes [30]. Such a possibility is at the moment under investigation.

ACKNOWLEDGMENTS

We wish to thank Oreste Nicosini for several fruitful discussions and suggestions.

APPENDIX: COMPLETE 1-LOOP ELECTROWEAK CONTRIBUTIONS TO $\tilde{\Delta}_{\alpha,EF}$, R_{EF} , $V_{EF}^{\gamma Z}$ AND $V_{EF}^{Z\gamma}$

We give here the explicit expressions of the quantities that appear in Eqs. (2.19)-(2.22).

1. Charged boson contributions

Universal self-energy WW components (Fig. 1):

$$\begin{aligned} \tilde{\Delta}_{\alpha,ef}^{s.e. (WW)}(q^2) = & -\left(\frac{5\alpha}{4\pi}\right)\left\{\int_0^1 dx \left[1 - \frac{12}{5}x(1-x)\right] \ln \left|1 - \frac{q^2}{M_W^2}x(1-x)\right| \right. \\ & \left. + \frac{4}{15} + \left(\frac{8M_W^2}{5q^2}\right) \int_0^1 dx \ln \left|1 - \frac{q^2}{M_W^2}x(1-x)\right|\right\} \end{aligned} \quad (A1)$$

$$\begin{aligned} R_{ef}^{s.e. (WW)}(q^2) = & -\left(\frac{\alpha}{4\pi}\right) \int_0^1 dx \left\{ \frac{2x(1-x)[20c^4 + (1-2s^2)^2] - 20c^4}{4c^2s^2} \left[\frac{q^2}{q^2 - M_Z^2} \mathcal{L} \right. \right. \\ & \left. \left. + \frac{x(1-x)M_Z^2}{M_W^2 - x(1-x)M_Z^2} \right] + 2M_W^2 \left(\frac{-17 + 36s^2 - 16s^4}{4c^2s^2} \right) \left[\frac{q^2}{q^2 - M_Z^2} \bar{\mathcal{L}} - M_Z^2 \mathcal{L}'_Z \right] \right\} \end{aligned} \quad (A2)$$

$$\mathcal{L} = \ln \left| \frac{M_W^2 - q^2x(1-x)}{M_W^2 - M_Z^2x(1-x)} \right| \quad (A3)$$

$$\bar{\mathcal{L}} = \frac{1}{q^2} \ln \left| 1 - \frac{q^2}{M_W^2}x(1-x) \right| - \frac{1}{M_Z^2} \ln \left| 1 - \frac{M_Z^2}{M_W^2}x(1-x) \right| \quad (A4)$$

$$\mathcal{L}'_Z = -\left(\frac{1}{M_Z^2}\right) \left[\frac{x(1-x)}{M_W^2 - M_Z^2x(1-x)} + \frac{1}{M_Z^2} \ln \left| 1 - \frac{M_Z^2}{M_W^2}x(1-x) \right| \right] \quad (A5)$$

$$\begin{aligned} V_{ef}^{s.e. (WW)}(q^2) = & -\left(\frac{\alpha}{4\pi}\right) \int_0^1 dx \left\{ \frac{1}{q^2} \left[\frac{8s^2 - 9}{cs} M_W^2 - 5\frac{c}{s}q^2 + \frac{11 - 12s^2}{cs}x(1-x)q^2 \right] \ln \left| 1 - \frac{q^2}{M_W^2}x(1-x) \right| \right. \\ & \left. - \left(\frac{1}{M_Z^2}\right) \left[\frac{8s^2 - 9}{cs} M_W^2 - 5\frac{c}{s}M_Z^2 + \frac{11 - 12s^2}{cs}x(1-x)M_Z^2 \right] \ln \left| 1 - \frac{M_Z^2}{M_W^2}x(1-x) \right| \right\} \end{aligned} \quad (A6)$$

WW vertex component (Fig. 2a, universal for light fermions)

$$\tilde{\Delta}_{\alpha,ef}^{vert. (WW)}(q^2) = -\left(\frac{\alpha}{\pi}\right) \int \int dx_1 dx_2 \left[3 \ln \left| 1 - \frac{q^2 x_1 x_2}{M_W^2 (x_1 + x_2)} \right| + \frac{q^2 (x_1 + x_2 - x_1 x_2)}{M_W^2 (x_1 + x_2) - q^2 x_1 x_2} \right] \quad (A7)$$

$$\begin{aligned} R_{ef}^{vert. (WW)}(q^2) = & \frac{\alpha}{\pi} \left(\frac{c^2}{s^2}\right) \int \int dx_1 dx_2 \left\{ 3 \ln \left| \frac{M_W^2 (x_1 + x_2) - q^2 x_1 x_2}{M_W^2 (x_1 + x_2) - M_Z^2 x_1 x_2} \right| \right. \\ & \left. + \frac{(q^2 - M_Z^2) M_W^2 (x_1 + x_2) (x_1 + x_2 - x_1 x_2)}{[M_W^2 (x_1 + x_2) - q^2 x_1 x_2][M_W^2 (x_1 + x_2) - M_Z^2 x_1 x_2]} \right\} \end{aligned} \quad (A8)$$

$$\begin{aligned}
V_{ef}^{vert. (WW)}(q^2) &= \frac{\alpha}{2\pi} \left(\frac{c}{s}\right) \int \int dx_1 dx_2 \left\{ 3 \ln \left| \frac{M_W^2(x_1+x_2) - q^2 x_1 x_2}{M_W^2(x_1+x_2) - M_Z^2 x_1 x_2} \right| \right. \\
&\quad + \frac{(q^2 - M_Z^2) M_W^2(x_1+x_2)(x_1+x_2 - x_1 x_2)}{[M_W^2(x_1+x_2) - q^2 x_1 x_2][M_W^2(x_1+x_2) - M_Z^2 x_1 x_2]} \\
&\quad \left. + \left(\frac{q^2 - M_Z^2}{q^2}\right) \left[3 \ln \left| 1 - \frac{q^2 x_1 x_2}{M_W^2(x_1+x_2)} \right| + \frac{q^2(x_1+x_2 - x_1 x_2)}{M_W^2(x_1+x_2) - q^2 x_1 x_2} \right] \right\}
\end{aligned} \tag{A9}$$

WW vertex component for $b\bar{b}$ final state

$$\begin{aligned}
\tilde{\Delta}_{\alpha,eb}^{vert. (WW)}(q^2) &= \frac{\alpha}{2\pi} \int \int dx_1 dx_2 \left(3 + \frac{m_t^2}{2M_W^2} \right) \ln \left| \frac{M_W^2(x_1+x_2) + m_t^2(1-x_1-x_2)}{M_W^2(x_1+x_2) + m_t^2(1-x_1-x_2) - q^2 x_1 x_2} \right| \\
&\quad - \frac{\alpha}{2\pi} \int \int dx_1 dx_2 \frac{q^2(x_1+x_2 - x_1 x_2)}{M_W^2(x_1+x_2) + m_t^2(1-x_1-x_2) - q^2 x_1 x_2} + \frac{1}{2} \tilde{\Delta}_{\alpha,e\mu}^{vert. (WW)}(q^2)
\end{aligned} \tag{A10}$$

$$\begin{aligned}
R_{eb}^{vert. (WW)}(q^2) &= \frac{\alpha}{8\pi s^2} \int \int dx_1 dx_2 \left\{ [12c^2 + (1-2s^2) \frac{m_t^2}{M_W^2}] \times \right. \\
&\quad \ln \left| \frac{M_W^2(x_1+x_2) + m_t^2(1-x_1-x_2) - q^2 x_1 x_2}{M_W^2(x_1+x_2) + m_t^2(1-x_1-x_2) - M_Z^2 x_1 x_2} \right| + 4c^2 \left[\frac{q^2(x_1+x_2 - x_1 x_2)}{M_W^2(x_1+x_2) + m_t^2(1-x_1-x_2) - q^2 x_1 x_2} \right. \\
&\quad \left. \left. - \frac{M_Z^2(x_1+x_2 - x_1 x_2)}{M_W^2(x_1+x_2) + m_t^2(1-x_1-x_2) - M_Z^2 x_1 x_2} \right] \right\} + \frac{1}{2} R_{e\mu}^{vert. (WW)}(q^2)
\end{aligned} \tag{A11}$$

$$\begin{aligned}
V_{eb}^{\gamma Z, vert. (WW)}(q^2) &= \frac{\alpha}{2\pi} \left(\frac{c}{s}\right) \int \int dx_1 dx_2 \left\{ 3 \ln \left| \frac{M_W^2(x_1+x_2) - q^2 x_1 x_2}{M_W^2(x_1+x_2) - M_Z^2 x_1 x_2} \right| \right. \\
&\quad + \frac{(q^2 - M_Z^2) M_W^2(x_1+x_2)(x_1+x_2 - x_1 x_2)}{[M_W^2(x_1+x_2) - q^2 x_1 x_2][M_W^2(x_1+x_2) - M_Z^2 x_1 x_2]} \\
&\quad + \frac{q^2 - M_Z^2}{q^2} \left(\frac{\alpha c}{2\pi s}\right) \int \int dx_1 dx_2 \left\{ 3 \ln \left| \frac{M_W^2(x_1+x_2) + m_t^2(1-x_1-x_2) - q^2 x_1 x_2}{M_W^2(x_1+x_2) + m_t^2(1-x_1-x_2)} \right| \right. \\
&\quad \left. \left. + \frac{q^2(x_1+x_2 - x_1 x_2)}{M_W^2(x_1+x_2) + m_t^2(1-x_1-x_2) - q^2 x_1 x_2} \right] \right\}
\end{aligned} \tag{A12}$$

$$\begin{aligned}
V_{eb}^{Z\gamma, vert. (WW)}(q^2) &= \frac{\alpha}{2\pi} \left(\frac{c}{s}\right) \int \int dx_1 dx_2 \\
&\quad \left(\frac{q^2 - M_Z^2}{q^2} \right) \left[3 \ln \left| 1 - \frac{q^2 x_1 x_2}{M_W^2(x_1+x_2)} \right| + \frac{q^2(x_1+x_2 - x_1 x_2)}{M_W^2(x_1+x_2) - q^2 x_1 x_2} \right] \\
&\quad + \left(\frac{\alpha}{8\pi s c}\right) \int \int dx_1 dx_2 \left\{ [12c^2 + (1-2s^2) \frac{m_t^2}{M_W^2}] \times \right. \\
&\quad \ln \left| \frac{M_W^2(x_1+x_2) + m_t^2(1-x_1-x_2) - q^2 x_1 x_2}{M_W^2(x_1+x_2) + m_t^2(1-x_1-x_2) - M_Z^2 x_1 x_2} \right| \\
&\quad \left. + 4c^2 \left[\frac{q^2(x_1+x_2 - x_1 x_2)}{M_W^2(x_1+x_2) + m_t^2(1-x_1-x_2) - q^2 x_1 x_2} - \frac{M_Z^2(x_1+x_2 - x_1 x_2)}{M_W^2(x_1+x_2) + m_t^2(1-x_1-x_2) - M_Z^2 x_1 x_2} \right] \right\}
\end{aligned} \tag{A13}$$

Single W vertex component (Fig. 2b, light fermions; non universal)

$$\tilde{\Delta}_{\alpha,eu}^{vert. (W)}(q^2, \theta) = \frac{\alpha}{6\pi} \int \int dx_1 dx_2 \left[\ln \left| 1 - \frac{q^2 x_1 x_2}{M_W^2(1-x_1-x_2)} \right| - \frac{q^2(1-x_1)(1-x_2)}{M_W^2(1-x_1-x_2) - q^2 x_1 x_2} \right] \tag{A14}$$

$$\tilde{\Delta}_{\alpha,ed}^{vert.(W)}(q^2, \theta) = 2\tilde{\Delta}_{\alpha,eu}^{vert.(W)}(q^2, \theta) \quad (\text{A15})$$

$$R_{e\mu}^{vert.(W)}(q^2) = \frac{\alpha}{2\pi s^2} \int \int dx_1 dx_2 \left\{ \ln \left| \frac{M_W^2(1-x_1-x_2) - M_Z^2 x_1 x_2}{M_W^2(1-x_1-x_2) - q^2 x_1 x_2} \right| \right. \\ \left. + \frac{(q^2 - M_Z^2) M_W^2 (1-x_1-x_2)(1-x_1)(1-x_2)}{[M_W^2(1-x_1-x_2) - q^2 x_1 x_2][M_W^2(1-x_1-x_2) - M_Z^2 x_1 x_2]} \right\} \quad (\text{A16})$$

$$R_{eu}^{vert.(W)}(q^2) = \left(1 - \frac{s^2}{3}\right) R_{e\mu}^{vert.(W)}(q^2) \quad (\text{A17})$$

$$R_{ed}^{vert.(W)}(q^2) = \left(1 - \frac{2s^2}{3}\right) R_{e\mu}^{vert.(W)}(q^2) \quad (\text{A18})$$

$$V_{e\mu}^{vert.(W)}(q^2) = \frac{\alpha}{4\pi c s} \int \int dx_1 dx_2 \left\{ \ln \left| \frac{M_W^2(1-x_1-x_2) - M_Z^2 x_1 x_2}{M_W^2(1-x_1-x_2) - q^2 x_1 x_2} \right| \right. \\ \left. + \frac{(q^2 - M_Z^2) M_W^2 (1-x_1-x_2)(1-x_1)(1-x_2)}{[M_W^2(1-x_1-x_2) - q^2 x_1 x_2][M_W^2(1-x_1-x_2) - M_Z^2 x_1 x_2]} \right\} \quad (\text{A19})$$

$$V_{eu}^{\gamma Z, vert.(W)}(q^2, \theta) = V_{e\mu}^{vert.(W)}(q^2) - \left(\frac{q^2 - M_Z^2}{q^2}\right) \left(\frac{\alpha c}{6\pi s}\right) \int \int dx_1 dx_2 \left\{ \right. \\ \left. \ln \left| 1 - \frac{q^2 x_1 x_2}{M_W^2(1-x_1-x_2)} \right| - \frac{q^2(1-x_1)(1-x_2)}{M_W^2(1-x_1-x_2) - q^2 x_1 x_2} \right\} \quad (\text{A20})$$

$$V_{ed}^{\gamma Z, vert.(W)}(q^2, \theta) = V_{e\mu}^{vert.(W)}(q^2) - \left(\frac{q^2 - M_Z^2}{q^2}\right) \left(\frac{\alpha c}{3\pi s}\right) \int \int dx_1 dx_2 \left\{ \right. \\ \left. \left\{ \ln \left| 1 - \frac{q^2 x_1 x_2}{M_W^2(1-x_1-x_2)} \right| - \frac{q^2(1-x_1)(1-x_2)}{M_W^2(1-x_1-x_2) - q^2 x_1 x_2} \right\} \right\} \quad (\text{A21})$$

$$V_{ed}^{Z\gamma, vert.(W)}(q^2, \theta) = \left(1 - \frac{4s^2}{3}\right) V_{e\mu}^{vert.(W)}(q^2) \quad (\text{A22})$$

$$V_{eu}^{Z\gamma, vert.(W)}(q^2, \theta) = \left(1 - \frac{2s^2}{3}\right) V_{e\mu}^{vert.(W)}(q^2) \quad (\text{A23})$$

Single W vertex component for $b\bar{b}$ final state

$$\tilde{\Delta}_{\alpha,lb}^{vert.(W)}(q^2) = \frac{\alpha}{3\pi} \left(1 + \frac{m_t^2}{2M_W^2}\right) \int \int dx_1 dx_2 \left\{ \ln \left| \frac{M_W^2(1-x_1-x_2) + m_t^2(x_1+x_2) - q^2 x_1 x_2}{M_W^2(1-x_1-x_2) + m_t^2(x_1+x_2)} \right| \right. \\ \left. + \frac{m_t^2}{M_W^2(1-x_1-x_2) + m_t^2(x_1+x_2)} - \frac{m_t^2 + q^2(1-x_1)(1-x_2)}{M_W^2(1-x_1-x_2) + m_t^2(x_1+x_2) - q^2 x_1 x_2} \right\} \quad (\text{A24})$$

$$R_{eb}^{vert.(W)}(q^2) = \frac{\alpha}{8\pi s^2} \int \int dx_1 dx_2 \left\{ \left[2\left(1 - \frac{4s^2}{3}\right) - \frac{4s^2 m_t^2}{3M_W^2} \right] \right. \\ \left. \left[-\ln \left| \frac{M_W^2(1-x_1-x_2) + m_t^2(x_1+x_2) - q^2 x_1 x_2}{M_W^2(1-x_1-x_2) + m_t^2(x_1+x_2) - M_Z^2 x_1 x_2} \right| \right. \right. \\ \left. \left. + \frac{q^2(1-x_1)(1-x_2)}{M_W^2(1-x_1-x_2) + m_t^2(x_1+x_2) - q^2 x_1 x_2} - \frac{M_Z^2(1-x_1)(1-x_2)}{M_W^2(1-x_1-x_2) + m_t^2(x_1+x_2) - M_Z^2 x_1 x_2} \right] \right. \\ \left. + \left[\left(1 - \frac{4s^2}{3}\right) \frac{m_t^2}{M_W^2} - \frac{8s^2}{3} \right] m_t^2 \left[\frac{1}{M_W^2(1-x_1-x_2) + m_t^2(x_1+x_2) - q^2 x_1 x_2} \right. \right. \\ \left. \left. - \frac{1}{M_W^2(1-x_1-x_2) + m_t^2(x_1+x_2) - M_Z^2 x_1 x_2} \right] \right\} + \frac{1}{2} R_{e\mu}^{vert.(W)}(q^2) \quad (\text{A25})$$

$$\begin{aligned}
V_{eb}^{\gamma Z, vert. (W)}(q^2) &= \frac{\alpha}{4\pi c s} \int \int dx_1 dx_2 \left\{ \ln \left| \frac{M_W^2(1-x_1-x_2) - M_Z^2 x_1 x_2}{M_W^2(1-x_1-x_2) - q^2 x_1 x_2} \right| \right. \\
&+ \left. \frac{(q^2 - M_Z^2) M_W^2(1-x_1-x_2)(1-x_1)(1-x_2)}{[M_W^2(1-x_1-x_2) - q^2 x_1 x_2][M_W^2(1-x_1-x_2) - M_Z^2 x_1 x_2]} \right\} \\
&+ \left(\frac{\alpha c}{3\pi s} \right) \frac{q^2 - M_Z^2}{q^2} \left(1 + \frac{m_t^2}{2M_W^2} \right) \int \int dx_1 dx_2 \left[-\ln \left| \frac{M_W^2(1-x_1-x_2) + m_t^2(x_1+x_2) - q^2 x_1 x_2}{M_W^2(1-x_1-x_2) + m_t^2(x_1+x_2)} \right| \right. \\
&+ \left. \frac{m_t^2 + q^2(1-x_1)(1-x_2)}{M_W^2(1-x_1-x_2) + m_t^2(x_1+x_2) - q^2 x_1 x_2} - \frac{m_t^2}{M_W^2(1-x_1-x_2) + m_t^2(x_1+x_2)} \right] \quad (A26)
\end{aligned}$$

$$\begin{aligned}
V_{eb}^{Z\gamma, vert. (W)}(q^2) &= \left(\frac{\alpha}{8\pi s c} \right) \left\{ \left[2\left(1 - \frac{4s^2}{3}\right) - \frac{8s^2 m_t^2}{3M_W^2} \right] \int \int dx_1 dx_2 \right. \\
&+ \left. \left[-\ln \left| \frac{M_W^2(1-x_1-x_2) + m_t^2(x_1+x_2) - q^2 x_1 x_2}{M_W^2(1-x_1-x_2) + m_t^2(x_1+x_2) - M_Z^2 x_1 x_2} \right| \right. \right. \\
&+ \left. \left. \frac{q^2(1-x_1)(1-x_2)}{M_W^2(1-x_1-x_2) + m_t^2(x_1+x_2) - q^2 x_1 x_2} - \frac{M_Z^2(1-x_1)(1-x_2)}{M_W^2(1-x_1-x_2) + m_t^2(x_1+x_2) - M_Z^2 x_1 x_2} \right] \right. \\
&+ \left. \left[\left(1 - \frac{4s^2}{3}\right) \frac{m_t^2}{M_W^2} - \frac{8s^2}{3} \right] \int \int dx_1 dx_2 m_t^2 \left[\frac{1}{M_W^2(1-x_1-x_2) + m_t^2(x_1+x_2) - q^2 x_1 x_2} \right. \right. \\
&+ \left. \left. \frac{1}{M_W^2(1-x_1-x_2) + m_t^2(x_1+x_2) - M_Z^2 x_1 x_2} \right] \right] \quad (A27)
\end{aligned}$$

2. Neutral boson effects

ZH self-energy (Fig. 4)

$$\begin{aligned}
R^{s.e. (ZH)}(q^2) &= \left(\frac{\alpha}{8\pi s^2 c^2} \right) \int_0^1 dx \left\{ [M_Z^2(x-2) + M_H^2(1-x)] \left[\frac{q^2}{q^2 - M_Z^2} \bar{\mathcal{H}} \right. \right. \\
&+ \left. \frac{x(1-x)}{M_Z^2 x^2 + M_H^2(1-x)} + \frac{1}{M_Z^2} \ln \left| 1 - \frac{M_Z^2 x(1-x)}{M_Z^2 x + M_H^2(1-x)} \right| \right] \\
&- \left. x(1-x) \left[\frac{q^2}{q^2 - M_Z^2} \mathcal{H} + \frac{x(1-x)M_Z^2}{M_Z^2 x^2 + M_H^2(1-x)} \right] \right\} \quad (A28)
\end{aligned}$$

$$\mathcal{H} \equiv \ln \left| \frac{M_Z^2 x + M_H^2(1-x) - q^2 x(1-x)}{M_Z^2 x^2 + M_H^2(1-x)} \right| \quad (A29)$$

$$\bar{\mathcal{H}} \equiv \frac{1}{q^2} \ln \left| 1 - \frac{q^2 x(1-x)}{M_Z^2 x + M_H^2(1-x)} \right| - \frac{1}{M_Z^2} \ln \left| 1 - \frac{M_Z^2 x(1-x)}{M_Z^2 x + M_H^2(1-x)} \right| \quad (A30)$$

Single Z triangle (Fig. 5)

$$\begin{aligned}
\tilde{\Delta}_{\alpha, ef}^{vert. (Z)}(q^2) &= \frac{\alpha(2 - v_e^2 - v_f^2)}{32\pi s^2 c^2} \int \int dx_1 dx_2 \left[-\ln \left| 1 - \frac{q^2 x_1 x_2}{M_Z^2(1-x_1-x_2)} \right| \right. \\
&+ \left. \frac{q^2(1-x_1)(1-x_2)}{M_Z^2(1-x_1-x_2) - q^2 x_1 x_2} \right] \quad (A31)
\end{aligned}$$

$$\begin{aligned}
R_{ef}^{vert. (Z)}(q^2) &= \frac{\alpha(2 + 3v_e^2 + 3v_f^2)}{32\pi s^2 c^2} \int \int dx_1 dx_2 \left[-\ln \left| \frac{M_Z^2(1-x_1-x_2) - q^2 x_1 x_2}{M_Z^2(1-x_1-x_2 - x_1 x_2)} \right| \right. \\
&+ \left. \frac{q^2(1-x_1)(1-x_2)}{M_Z^2(1-x_1-x_2) - q^2 x_1 x_2} - \frac{(1-x_1)(1-x_2)}{1-x_1-x_2-x_1 x_2} \right] \quad (A32)
\end{aligned}$$

$$\begin{aligned}
V_{ef}^{\gamma Z, vert. (Z)}(q^2) &= \left(\frac{\alpha v_e (1 - v_e^2)}{64\pi s^3 c^3} \right) \int \int dx_1 dx_2 \left[-\ln \left| \frac{M_Z^2 (1 - x_1 - x_2) - q^2 x_1 x_2}{M_Z^2 (1 - x_1 - x_2 - x_1 x_2)} \right| \right. \\
&\quad \left. + \frac{q^2 (1 - x_1)(1 - x_2)}{M_Z^2 (1 - x_1 - x_2) - q^2 x_1 x_2} - \frac{(1 - x_1)(1 - x_2)}{1 - x_1 - x_2 - x_1 x_2} \right] \\
&\quad - \frac{q^2 - M_Z^2}{q^2} \left(\frac{\alpha |Q_f| v_f}{4\pi s c} \right) \int \int dx_1 dx_2 \left[-\ln \left| 1 - \frac{q^2 x_1 x_2}{M_Z^2 (1 - x_1 - x_2)} \right| \right. \\
&\quad \left. + \frac{q^2 (1 - x_1)(1 - x_2)}{M_Z^2 (1 - x_1 - x_2) - q^2 x_1 x_2} \right]
\end{aligned} \tag{A33}$$

$$\begin{aligned}
V_{ef}^{Z\gamma, vert. (Z)}(q^2) &= \left(\frac{\alpha v_f (1 - v_f^2)}{64|Q_f|\pi s^3 c^3} \right) \int \int dx_1 dx_2 \left[-\ln \left| \frac{M_Z^2 (1 - x_1 - x_2) - q^2 x_1 x_2}{M_Z^2 (1 - x_1 - x_2 - x_1 x_2)} \right| \right. \\
&\quad \left. + \frac{q^2 (1 - x_1)(1 - x_2)}{M_Z^2 (1 - x_1 - x_2) - q^2 x_1 x_2} - \frac{(1 - x_1)(1 - x_2)}{1 - x_1 - x_2 - x_1 x_2} \right] \\
&\quad - \frac{q^2 - M_Z^2}{q^2} \left(\frac{\alpha v_e}{4\pi s c} \right) \int \int dx_1 dx_2 \left[-\ln \left| 1 - \frac{q^2 x_1 x_2}{M_Z^2 (1 - x_1 - x_2)} \right| \right. \\
&\quad \left. + \frac{q^2 (1 - x_1)(1 - x_2)}{M_Z^2 (1 - x_1 - x_2) - q^2 x_1 x_2} \right]
\end{aligned} \tag{A34}$$

3. Box diagrams

In the light fermionic case the WW and ZZ box amplitudes have been written in Ref. [14] in terms of I and I_5 functions. We have also written them in the Passarino-Veltman description [31] in terms of D_i functions as defined in Ref. [32]. We have checked [33] that both expressions agree numerically using the package of Ref. [34]. The extension to the bb case could be done very easily by just putting $m = m_t$ instead of $m = 0$ inside $D_i(0, 0, 0, 0, t, q^2; M, 0, m, M)$. Projecting these amplitudes on photon and Z structures then give the following results.

WW box (Fig. 3)

Defining from Fig. 3a

$$D_\mu^W = D_d^W \equiv [D_{27} - \frac{t}{2}(D_{25} - D_{24} - D_{11})] = \frac{[I(q^2, t, M_W) + I_5(q^2, t, M_W)]}{2q^2} \tag{A35}$$

and from Fig. 3b (\bar{D} having the meaning of changing t into u inside D)

$$\begin{aligned}
D_u^W &\equiv [4\bar{D}_{27} + \frac{q^2}{2}(\bar{D}_{13} + 2\bar{D}_{26}) + \frac{t}{2}(\bar{D}_{13} + 2\bar{D}_{25}) + \frac{u}{2}(\bar{D}_{11} + \bar{D}_{12} + 2\bar{D}_{24})] \\
&= \frac{[I(q^2, u, M_W) - I_5(q^2, u, M_W)]}{2q^2}
\end{aligned} \tag{A36}$$

we obtain:

$$\tilde{\Delta}_{\alpha, ef}^{(Box, WW)}(q^2, \theta) = \frac{\alpha q^2}{16\pi |Q_f| s^4} (1 - v_e)(1 - v_f) D_f^W \tag{A37}$$

$$R_{ef}^{(Box, WW)}(q^2, \theta) = \frac{c^2 (M_Z^2 - q^2) \alpha}{\pi s^2} D_f^W \tag{A38}$$

$$V_{ef}^{\gamma Z (Box, WW)}(q^2, \theta) = \frac{c(M_Z^2 - q^2)(1 - v_e)\alpha}{4\pi s^3} D_f^W \tag{A39}$$

$$V_{ef}^{Z\gamma (Box, WW)}(q^2, \theta) = \frac{c(M_Z^2 - q^2)(1 - v_f)\alpha}{4\pi |Q_f| s^3} D_f^W \tag{A40}$$

ZZ box (Fig. 6)

For the ZZ box, we obtain

$$\tilde{\Delta}_{\alpha,ef}^{(Box,ZZ)}(q^2, \theta) = -\left(\frac{\alpha q^2}{256\pi Q_f s^4 c^4}\right)[(1-v_e^2)(1-v_f^2)D_1^Z + v_e v_f(1-v_e^2)(1-v_f^2)D_2^Z] \quad (\text{A41})$$

$$R_{ef}^{(Box,ZZ)}(q^2, \theta) = -I_{3f} \frac{\alpha(M_Z^2 - q^2)}{8\pi s^2 c^2} [4v_e v_f D_1^Z + (1+v_e^2)(1+v_f^2)D_2^Z] \quad (\text{A42})$$

$$V_{ef}^{\gamma Z (Box,ZZ)}(q^2, \theta) = -I_{3f} \frac{\alpha(M_Z^2 - q^2)}{32\pi s^3 c^3} [2v_f(1-v^2)D_1^Z + v_e(1-v_e^2)(1+v_f^2)D_2^Z] \quad (\text{A43})$$

$$V_{ef}^{Z\gamma (Box,ZZ)}(q^2, \theta) = -\left(\frac{\alpha(M_Z^2 - q^2)}{64\pi Q_f s^3 c^3}\right)[2v_e(1-v_f^2)D_1^Z + v_f(1+v_e^2)(1-v_f^2)D_2^Z] \quad (\text{A44})$$

with

$$\begin{aligned} D_1^Z &\equiv [D_{27} + \frac{(t-u)}{4}(D_{24} - D_{25} + D_{11}) \\ &- [4\bar{D}_{27} + \frac{q^2}{2}(\bar{D}_{13} + 2\bar{D}_{26}) + \frac{t}{2}(\bar{D}_{13} + 2\bar{D}_{25}) + \frac{u}{2}(\bar{D}_{11} + \bar{D}_{12} + 2\bar{D}_{24})] \\ &= \frac{[I(q^2, t, M_Z) - I(q^2, u, M_Z)]}{2q^2} \end{aligned} \quad (\text{A45})$$

$$D_2^Z \equiv \left(\frac{q^2}{4}\right)[D_{25} - D_{24} - D_{11}] = \frac{[I_5(q^2, t, M_Z) + I_5(q^2, u, M_Z)]}{2q^2} \quad (\text{A46})$$

4. Fermion pair component

The contribution from Fig. 7 is universal and leads to (m_f being the mass of the fermion in the loop, $g_{Vf} = v_f I_{3f}$, $g_{Af} = I_{3f}$):

$$\tilde{\Delta}_{\alpha}^{s.e. (f\bar{f})}(q^2) = \frac{\alpha Q_f^2}{\pi} \int_0^1 dx \, 2x(1-x) \ln |1 - \frac{q^2}{m_f} x(1-x)| \quad (\text{A47})$$

$$\begin{aligned} R^{s.e. (f\bar{f})}(q^2) &= \left(\frac{\alpha}{4\pi s^2 c^2}\right) \int_0^1 dx \, \{2m_f^2 g_{Af}^2 [\frac{q^2}{q^2 - M_Z^2} \bar{J} \\ &+ \frac{x(1-x)}{m_f^2 - M_Z^2 x(1-x)} + \frac{1}{M_Z^2} \ln |1 - \frac{M_Z^2}{m_f} x(1-x)|] \\ &- 2(g_{Vf}^2 + g_{Af}^2)x(1-x) [\frac{q^2}{q^2 - M_Z^2} J + \frac{x(1-x)M_Z^2}{m_f^2 - M_Z^2 x(1-x)}]\} \end{aligned} \quad (\text{A48})$$

$$J \equiv \ln \left| \frac{m_f^2 - q^2 x(1-x)}{m_f^2 - M_Z^2 x(1-x)} \right| \quad (\text{A49})$$

$$\bar{J} \equiv \frac{1}{q^2} \ln |1 - \frac{q^2}{m_f^2} x(1-x)| - \frac{1}{M_Z^2} \ln |1 - \frac{M_Z^2}{m_f^2} x(1-x)| \quad (\text{A50})$$

$$V^{s.e. (f\bar{f})}(q^2) = -\left(\frac{\alpha Q_f g_{Vf}}{2\pi s c}\right) \int_0^1 dx \, 2x(1-x) \ln \left| \frac{m_f^2 - q^2 x(1-x)}{m_f^2 - M_Z^2 x(1-x)} \right| \quad (\text{A51})$$

- [1] For recent reviews see e.g. G. Montagna, O. Nicrosini and F. Piccinini, “Precision Physics at LEP”, FNT/T 97/19, hep-ph/9802302, to appear in Riv. Nuovo Cim.; M. Martinez, R. Miquel, L. Rolandi and R. Tenchini, “Precision Tests of the Electroweak Interaction at the Z pole”, CERN-EP/98-27.
- [2] F. Jegerlehner, Z. f. Phys. C **32**, 195 (1986); B.W. Lynn, G. Penso and C. Verzegnassi, Phys. Rev. D **35**, 42 (1987); H. Burkhardt, F. Jegerlehner, G. Penso and C. Verzegnassi, Z. f. Phys. C **43**, 497 (1989); F. Jegerlehner, Prog. Part. Nucl. Phys. **27**, 32 (1991); M.L. Swartz, SLAC-PUB-6710 (1994) and Phys. Rev. D **53**, 5268 (1996); A.D. Martin and D. Zeppenfeld, Phys. Lett. B **345**, 558 (1995); R.B. Nevzorov, A.V. Novikov, M.L. Vysotsky, hep-ph/9405390; H. Burkhardt and B. Pietrzyk, Phys. Lett. B **356**, 398 (1995); S. Eidelman and F. Jegerlehner, Z. f. Phys. C **67**, 585 (1995).
For very recent determinations see: R. Alemany, M. Davier and A. Höcker, Eur. Phys. J. C **2**, 123 (1998); N.V. Krasnikov and R. Rodenberg, hep-ph/9711367; M. Davier and A. Höcker, hep-ph/9801361; J.H. Kühn and M. Steinhauser, hep-ph/9802241.
- [3] M. Veltman, Nucl. Phys. B **123**, 89 (1977).
- [4] A.A. Akhundov et al, Nucl. Phys. B **276**, 1 (1988); F. Diakonov and W. Wetzel, HD-THEP-88-4(1988); W. Beenakker and H. Hollik, Z. f. Phys. C **40**, 569 (1988); B.W. Lynn and R.G. Stuart, Phys. Lett. B **252**, 676 (1990); J. Bernabeu, A. Pich and A. Santamaria, Phys. Lett. B **200**, 569 (1988); Nucl. Phys. B **363**, 326 (1991); A. Blondel, A. Djouadi and C. Verzegnassi, Phys. Lett. B **293**, 253 (1992).
- [5] See e.g. F. Boudjema, B. Mele et al., “Standard Model Processes”, in *Physics at LEP2*, CERN Report 96-01, (Geneva, 1996), Vol. 1, p. 207, edited by G. Altarelli, T. Sjöstrand and F. Zwirner.
- [6] “ e^+e^- Collisions at 500 GeV: The Physics Potential”, *Proceedings of the Workshop-Munich, Annecy, Hamburg*, DESY 92-123A (1992), 92-123B (1992), 93-123C (1993), edited by P.M. Zerwas; E. Accomando et al., “Physics with e^+e^- Linear Colliders”, *Proceedings of the ECFA/DESY LC Physics Working Group*, DESY-97-100, hep-ph/9705442.
- [7] E.A. Kuraev and V.S. Fadin, Sov. J. Nucl. Phys. **41**, 466 (1985); G. Altarelli and G. Martinelli, in *Physics at LEP*, CERN Report 86-02 (Geneva, 1986), Vol. 1, p. 47, edited by J. Ellis and R. Peccei; O. Nicrosini and L. Trentadue, Phys. Lett. B **196**, 551 (1987); Z. f. Phys. C **39**, 479 (1988).
For reviews see also: O. Nicrosini and L. Trentadue, in *Radiative Corrections for e^+e^- Collisions*, edited by J.H. Kühn (Springer, Berlin, 1989), p. 25; in *QED Structure Functions*, edited by G. Bonvicini, AIP Conf. Proc. No. 201 (AIP, New York, 1990), p. 12; O. Nicrosini, *ibid.*, p. 73.
- [8] F.M. Renard and C. Verzegnassi, Phys. Rev. D **52**, 1369 (1995).
- [9] F.M. Renard and C. Verzegnassi, Phys. Rev. D **53**, 1290 (1996).
- [10] A. Blondel, F.M. Renard, L. Trentadue and C. Verzegnassi, Phys. Rev. D **54**, 5567 (1996).
- [11] R.S. Chivukula, F.M. Renard and C. Verzegnassi, Phys. Rev. D **57**, 2760 (1998).
- [12] G. Degrassi and A. Sirlin, Nucl. Phys. B **383**, 73 (1992).
- [13] G. Degrassi and A. Sirlin, Phys. Rev. D **46**, 3104 (1992).
- [14] See e.g. M. Consoli, W. Hollik and F. Jegerlehner, “Electroweak Radiative Corrections for Z Physics”, in *Z Physics at LEP1*, CERN Report 89-08, (Geneva, 1989), Vol. 1, p. 7, edited by G. Altarelli, R. Kleiss and C. Verzegnassi.
- [15] F.M. Renard and C. Verzegnassi, Phys. Rev. D **55**, 4370 (1997).
- [16] NAG Fortran Library Manual Mark 17 (Numerical Algorithms Group, Oxford, 1991).
- [17] G. Montagna, O. Nicrosini, G. Passarino and F. Piccinini, “TOPAZ0 4.0 - A New Version of a Computer Program for Evaluation of Deconvoluted and Realistic Observables at LEP1 and LEP2”, FNT/T 98/02, hep-ph/9804211; Comput. Phys. Commun. **93**, 120 (1996); G. Montagna, O. Nicrosini, G. Passarino, F. Piccinini and R. Pittau, Comput. Phys. Commun. **76**, 328 (1993).
- [18] R. Clare, “LEP Electroweak Physics Results”, talk given at the Zeuthen Workshop on Elementary Particle Theory, *Loops and Legs in Gauge Theories*, Rheinsberg, April 19-24, 1998, to appear in the Proceedings.
- [19] See e.g. P. Chiappetta, C. Verzegnassi et al., “Z’ Physics”, in *Physics at LEP2*, CERN Report 96-01, (Geneva, 1996), Vol. 1, p. 577, edited by G. Altarelli, T. Sjöstrand and F. Zwirner.
- [20] J.M. Cornwall, Phys. Rev. D **26**, 1453 (1982); J.M. Cornwall and J. Papavassiliou, Phys. Rev. D **40**, 3474 (1989).
- [21] M. Kuroda, G. Moulataka and D. Schildknecht, Nucl. Phys. B **350**, 25 (1991).
- [22] V.V. Sudakov, Sov. Phys. JETP **3**, 65 (1956).
- [23] G. Montagna, O. Nicrosini and F. Piccinini, Phys. Rev. D **48**, 1021 (1993).
- [24] G. Montagna, O. Nicrosini and F. Piccinini, Phys. Lett. B **406**, 243 (1997) and references therein.
- [25] F.A. Berends, G. Burgers and W.L. van Neerven, Nucl. Phys. B **297**, 429 (1988).
- [26] F.A. Berends et al., “Z Line Shape”, in *Z Physics at LEP1*, CERN Report 89-08, (Geneva, 1989), Vol.1, p.89, edited by G. Altarelli, R. Kleiss and C. Verzegnassi.
- [27] M. Böhm, W. Hollik et al., “Forward-backward asymmetries”, in *Z Physics at LEP1*, CERN Report 89-08, (Geneva, 1989), Vol.1, p.203, edited by G. Altarelli, R. Kleiss and C. Verzegnassi.
- [28] D. Bardin et al., Nucl. Phys. B **351**, 1 (1991).
- [29] W. Beenakker, F.A. Berends and W.L. van Neerven, in *Radiative Corrections for e^+e^- Collisions*, edited by J.H. Kühn, (Springer, Berlin, 1989), p. 3.
- [30] J. Layssac, F.M. Renard and C. Verzegnassi, Phys. Lett. B **418**, 134 (1998).

- [31] G. Passarino and M.Veltman, Nucl. Phys. B **160**, 151 (1979).
- [32] K. Hagiwara, S. Matsumoto, D. Haidt and C.S. Kim, Z. f. Phys. C **64**, 559 (1995).
- [33] J. Layssac, private communication.
- [34] Rolf Mertig, Guide to FeynCalc (1992).